Electrospun SnO_2/LTO Composite Sub-Micron Dimpled Spheres as High Performance Anode Material for Lithium Ion Batteries

Anulekha. K. Haridas [a, b, #], Chandra S. Sharma[a*], Tata N. Rao[b*]

[a]Creative & Advanced Research Based On Nanomaterials (CARBON) Laboratory, Department of Chemical Engineering, Indian Institute of Technology Hyderabad, Medak-502285, Telangana, India
[b]International Advanced Research Center for Powder Metallurgy and New Materials (ARCI), Hyderabad- 500005, Telangana, India

SnO_2 is one of the high capacity (782 mAh/g) anode materials used in lithium ion batteries with a tetragonal rutile structure and it alloys at voltage of 0.5V *vs* Li. However, cyclic stability for SnO_2 and Sn based materials is very poor due to high volume expansion during alloying with Li ions (charging) and disintegration of structure during de-alloying (discharging) besides the formation of solid electrolyte interface (SEI) at lower operating voltage of the anode. Many attempts have been made to improve the cycle stability and minimize capacity losses of these materials by nanostructuring, making nanocomposites with graphene and CNT. Even though the results are promising, reproducibility and the scaling up of the electrode material still remains as a challenge. Here we introduce electrospinning as a new way of improving the cycle stability with minimum capacity loss using a composite electrode of SnO_2 and lithium titanate (LTO). LTO with a cubic spinel structure can intercalate reversibly with Li ions delivering a capacity of 175 mAh/g, theoretically. Low crystal strains during charging–discharging makes the material work even at high charging rates. The combination of SnO_2 and LTO can reduce the volume expansion experienced by bare SnO_2 during alloying de-alloying reaction as LTO itself is a zero-strain material.

[*]**Corresponding Authors E- mail address:** cssharma@iith.ac.in, tata@arci.res.in
[#]**Author's Present address**: Department of Chemical and Bio Molecular Engineering, Rice University, Houston, 77005, Texas, United States

Introduction

Sn and SnO_2 based Lithium ion battery anodes have gathered great attention based on their high-energy densities basically due to the moderate voltage of operation (0.5V/Li) and high theoretical capacities (SnO_2 782 mAh/g, Sn 992 mAh/g) in comparison with the commercial graphite anode (372 mAh/g) [1-7]. Besides the high theoretical capacity, the material (Sn/ SnO_2) undergoes huge volume expansion (300 %) and contraction during Li- insertion and desertion respectively, leading to rapid capacity fading [8-10]. In comparison with Sn, oxides of Sn (SnO, SnO_2) on cycling with Li forms less solid electrolyte interface (SEI) and hence less Li loss that is related to a low capacity loss in the first cycle. Moreover, in the initial discharge cycle, as Li goes out of the material (de-

alloying) the SnLi alloy structure disintegration causes the formation of tiny Sn particles in a matrix of Li_2O that further engage in Li alloying /de-alloying reactions. The Li_2O formed in the first cycle can act as a conducting matrix enhancing the kinetics of Li ion transport during the successive charge discharge cycles.

Further, in order to tackle the inherent capacity fade allied due to the huge volume expansion and contraction in the lithiation and de-lithiation of SnO_2 anode, several structural modifications have been explored. Among those, carbon based composite electrode preparation utilizing graphene, CNTs, graphite and mesoporous carbons has gained much importance as those composites could considerably minimize the capacity fade in the Sn based electrode materials [11-17]. Another approach is the incorporation of another electrochemically active/ inactive oxide phase along with the SnO_2 anodes. The presence of second oxide phase has reported to reduce the capacity fade in comparison to the neat SnO_2 electrode materials [18-28].

By considering the above-mentioned points, here we present a composite SnO_2LTOC electrode material, synthesized by sol-gel/ electrospraying technique in the form of dimpled spheres. The presence of LTO in the composite electrode material is supposed to improve the capacity retention as it is a zero-strain material for the lithiation- delithiation mechanism [28]. More over conductive carbon in the electrode material enhances the Li ion diffusion provides high rate performance. The synthesis, characterization and electrochemical studies of the same are discussed in the coming sections.

Experimental

Materials

Titanium (IV) isopropoxide (TIP) 97% and Tin (IV) isopropoxide (SnIP) 10 wt/v in isopropanol were purchased from Alfa Aesar, India. Ethanol (99% pure), Lithium acetate di hydrate, Tin 2 ethyl hexanoate (T-2EH) and Polyethylene oxide (PEO, Mw 90,000 g/mol) were obtained from Sigma Aldrich, India. All the chemicals were used as such without any modification.

Preparation of SnO_2/LTO dimpled spheres by sol-gel/electrospinning

Initially LTO sol and SnO_2 sol were prepared separately similar to our earlier reported works [28, 29,30] and mixed in 1:2 ratio to make the precursor sol for SnO_2LTO DS. For preparing SnO_2 sol [28], 1 ml acetyl acetone was added to 2 ml ethanol and mixed thoroughly. SnIP was added to the above solution and was stirred for 30 min followed by drop wise addition of 500 µl water. To the above sol, T-2 EH was added to the aged sol, stirred for 30 min. 0.2% PEO solution was prepared in ethanol. The concentration Sn precursors in the SnO_2 sol were 33% (v/v) SnIP and 13% (v/v) T-2EH. LTO sol was prepared using TIP and lithium acetate di hydrate in Li: Ti ratio 4: 5 [29, 30]. Then the SnO_2 sol and LTO sol were mixed in 1:2 ratios by stirring for 1 h. Later the above solution was mixed with the PEO solution and electro-sprayed into SnO_2LTO dimpled spheres.

E-spin Nano machine, India was used for electrospinning process using 10 ml syringes fitted with 21 gauge needles. A voltage of 25 kV and 10 cm distance between the electrodes were maintained during electrospraying process. An aluminium foil was

used for collecting the electrosprayed precursor dimpled spheres. A part of these SnO_2LTOPEO precursor dimpled spheres were then calcined in air at 750 °C for 1 h to obtain SnO_2LTO-DS. Another part of SnO_2LTOPEO precursor dimpled spheres were annealed in argon atmosphere at 650 °C for 4 h to obtain SnO_2LTOC-DS dimpled spheres.

Characterization

Morphology and phase formation of the dimpled spheres calcined in air and argon atmospheres respectively were analyzed using Field Emission Scanning Electron Microscope (FESEM, Hitachi model- S4300SE/N).and X- ray Diffraction studies (XRD, Bruker D8 with Cu Ka radiation). Raman analysis (Lab Ram micro Raman) was also performed for understanding the presence of carbon in the dimpled spheres.

Electrode preparation and electrochemical testing

For preparing electrodes, slurries of SnO_2LTO-DS and SnO_2LTOC-DS were prepared by mixing 80 wt. % active materials with 10 wt. % PVDF and 10 wt. % conductive carbons in sufficient amounts of N- methyl pyrrolidone. The slurry was then coated on to Al foil using doctor blade with 30 µm thicknesses and then dried in vacuum oven for 20 h. The dried film was then cut into 12 mm discs using a disk cutter and assembled into coin cells in argon atmosphere. For assembling the coin cells, a Whatman micro glass separator, counter electrode (Li foil) and electrolyte (1M $LiPF_6$ in EC: DMC (1:1)) were used in cell assembling. Arbin Battery tester was used for testing the prepared coin cells.

Cyclic Voltammetry (CV) studies were conducted from 0.05 V to 2 V at a scan rate of 0.05 mV/s to understand the electrochemical reactions inside the SnO_2LTO-DS and SnO_2LTOC-DS. Later Galvanostatic charge discharge studies (GCD) were done in the potential range of 0.05 to 1.5 V at varying charging rates viz. 0.1 C, 0.3 C, 0.5 C, 0.8 C 1C, 3 C and 5 C for 10 cycles each to understand the rate performance of SnO_2LTO-DS and SnO_2LTOC-DS. Later cycle stability studies were conducted on the SnO_2LTOC-DS for 200 cycles at a higher charging rate of 1C.

Results and discussions

Morphology and Phase analysis

The morphology of the prepared dimpled spheres calcined in air and argon atmospheres are provided in the Figure 1. The air treated DS and argon tested DS were observed with 5µm in size and the high magnification image of both were observed with tiny grains of SnO_2 and The XRD analysis of SnO_2LTO-DS heat treated in air and argon atmospheres are provided in the Figure2. The XRD patterns (Figure.2A) revealed the presence of both SnO_2 and LTO phases and are matched with the JCPDS data cards in Match software for SnO_2 cassiterite phase (represented as $) and LTO spinel phase (denoted as *). The Raman analysis of dimpled spheres heat treated in argon revealed the presence of sharp D band and G band indicating the presence of carbon, along with the SnO_2 and LTO peaks (Figure.2B).

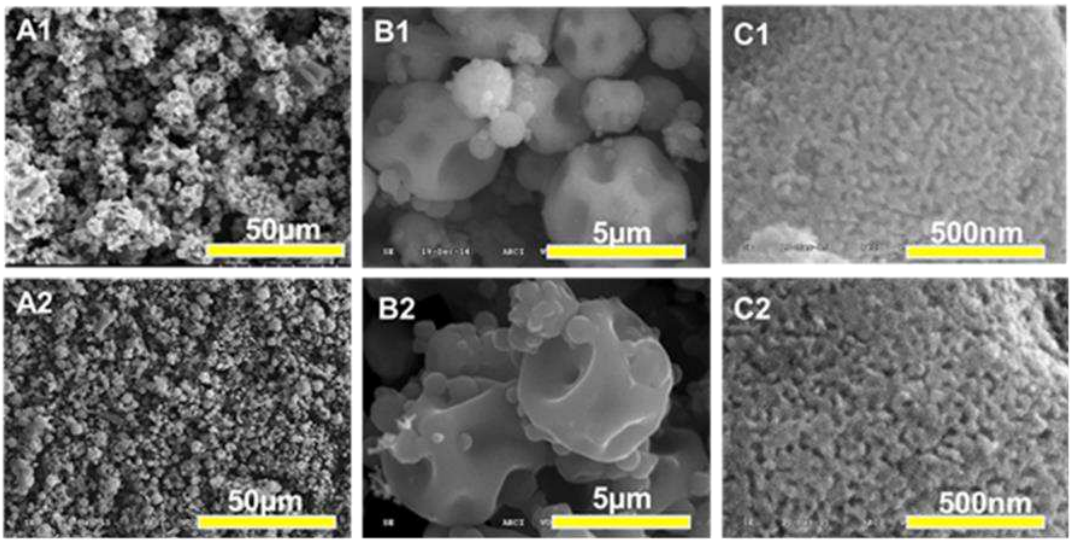

Figure1. A1, B1, C1 are FESEM images of SnO_2LTOC-DS whereas A2, B2, C2 are the FESEM images of SnO_2LTO-DS. D and E in the figure respectively represents the XRD patterns Raman spectra of both types of dimpled spheres

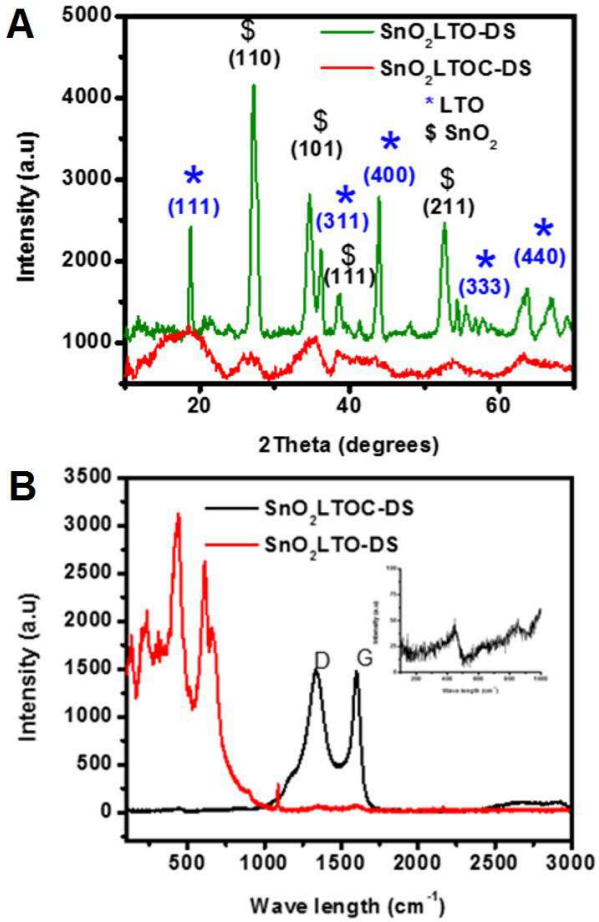

Figure2. XRD patterns (A) and Raman spectra (B) of both SnO_2LTO-DS and SnO_2LTOC-DSsamples

Cyclic voltammetry studies

The Cyclic voltammograms of SnO_2LTO and SnO_2LTOC- DS are represented in the Figure 3 (A, B). The initial discharge (de-lithiation) of SnO_2LTO-DS and SnO_2LTOC- DS half cells revealed the presence of cathodic peaks at 1.56, 1.4, 1, 0.5 and 0.3 and 0.2V respectively. During the cell charging (de-lithiation), anodic peaks were observed at 0.5V, 1V and 1.58 respectively. The cathodic peaks observed at 0.2V and the anodic peaks seen at 0.5V were observed in the subsequent CV cycles of both types of cells. The peaks observed at 1.56 V (cathodic) and 1.58 V (anodic) in the initial cycle can be attributed to the de-lithiation and lithiation reaction occurring in $Li_4Ti_5O_{12}$ crystals representing the reduction of Ti oxidation state from 3^+ to 4^+ whereas, the peaks observed at 0.2 V and 0.5 V represents the Sn-Li alloy –de alloy reaction in the Sn lattice [28, 31, 32, 33]. The rest of the peaks observed in the initial discharge cycle can be attributed to the irreversible SEI layer formed on the electrode due to the electrolyte decomposition [32, 33].Based on the above explanation, the reaction mechanism observed in the two types of electrodes can be depicted as below.

$$Li_4Ti_5O_{12} + 4.5Li + 4e \longrightarrow Li_{8.5}Ti_5O_{12} \quad \text{Scheme 1}$$

$$SnO_2 + 2Li + 2e \longrightarrow SnO + Li_2O \quad \text{Scheme 2}$$

$$SnO + 2Li + 2e \longrightarrow Sn + Li_2O \quad \text{Scheme 3}$$

$$Sn + xLi + xe \rightleftharpoons SnLi_x \quad \text{Scheme 4}$$

Hence, from the CV pattern obtained in the initial 5 cycles, it can be inferred that the SnO_2LTO and SnO_2LTOC electrodes undergoes a combination of electrode mechanism viz, intercalation and alloy/de-alloy in the initial cycle. Later, only Sn alloying-dealloying reaction persists in the following cycles and is the key mechanism contributing the electrode capacity [28].

Galvanostatic charge-discharge studies

As a comparative GCD study, Half-cells of SnO_2 powders, SnO_2LTO and SnO_2LTOC dimpled spheres were galvanostatically cycled from 0.05 to 1.5 V at 0.1C for 10 cycles. The voltage profiles of the same are represented respectively in C, D and E of Figure 3. SnO2 powders showed very poor performance with capacity fade reaching to 0 mAh/g in the initial 10 cycles. SnO_2LTO and SnO_2LTOC-DS have delivered an initial capacity of 1618 mAh/g and 1782 mAh/g respectively. At the end of the initial 10 cycles at 0.1C, SnO2LTO and SnO2LTOC-DS delivered capacities 300 mAh/g and 517 mAh/g respectively. Later Half cells of SnO_2LTO and SnO_2LTOC dimpled spheres were galvanostatically cycled at various current densities *viz.* 0.1C, 0.3 C, 0.5 C, 0.8 C, 1C, 3C and again back to 0.1C (for about 10 cycles each) for studying the rate capability (Figure 3 F, G) in them. At the lower C rate of 0.1C, the percentage capacity loss in the initial 10 cycles of both SnO_2LTO and SnO_2LTOC can be calculated as 81.5 and 71% respectively which is attributed to the volume expansion and crystal structure disintegration associated with Sn based materials. As the charging rates were increased, the capacity values were observed as reducing subsequently, whereas the cycle stabilities of the cells were observed as increasing as the charging rates were increased. This can be related as follows: At a lower charging rate, the electrode is utilized more for alloy/ de-alloy reaction as the kinetics of Li –alloying is slow. This leads to the formation of thicker solid electrolyte interface and more amount of SnLi crystal disintegration, due the slow reaction rate. At a higher charging rate, that is related with fast alloying de-alloying

reaction, due to the fast reaction rates the amount of Li loss in SEI is lesser. Table.1 shows a summary of the rate capability studies of SnO_2LTO and SnO_2LTOC-DS at various C rates. At the end of rate capability studies, SnO_2LTO and SnO_2LTOC-DS exhibited capacity values 0 mAh/g and 191 mAh/g respectively, ensuing almost 100 % and 88 % capacity loss from the initial cycle.

The SnO_2LTOC-DS was tested for cycle stability at 1C rate followed by the rate capability studies at a higher charging rate of 1C. At the end of 200 cycles, the cell has retained a capacity of 93 mAh/g and the percentage capacity loss associated with the cycle stability studies alone was calculated as 56%. The coulombic efficiency of the entire 200 cycles was calculated as 99%. When compared with a bare SnO_2 powders, the capacity retention in the SnO_2LTOC-DS were better. By carefully controlling the SnO_2 and LTO content in the DS and also by reducing the particle size of the dimpled spheres, the capacity fade in the same can be controlled in a more effective manner.

Conclusions

SnO_2LTO composite dimpled spheres were successfully prepared by using sol-gel assisted electrospraying technique with Sn: LTO ratio as 2:1. Two different atmospheric heat treatments (air and argon) yielded SnO_2LTO and SnO_2LTOC-DS. The composite electrode preparation with a second oxide phase has reduced the particle size in the resulting material enabled ease of Li -ion diffusion in the electrode. The SnO_2LTOC dimpled spheres showed superior electrochemical properties when compared with SnO_2LTO-DS and SnO_2 powders. A composite electrode architecture in the form of DS with small amount of conductive carbon as in (SnO_2LTOC DS) has helped in enhancing the electrochemical performance of the Sn based electrodes, by reducing the crystal structure disintegration during the alloy/de- alloy reactions. Further studies have to be done in optimizing the ratio of Sn and LTO in the composite electrode for obtaining better capacity retention and cyclic stability.

Acknowledgments

The authors extend their sincere thanks to Department of Science and Technology (DST), Nano Mission, India for the entire work. CSS acknowledges SERB Indo-Us Fellowship for presenting this work to 231st ECS Meeting in New Orleans. We also acknowledge Dr B.V Sarada ARCI, Hyderabad for Raman studies.

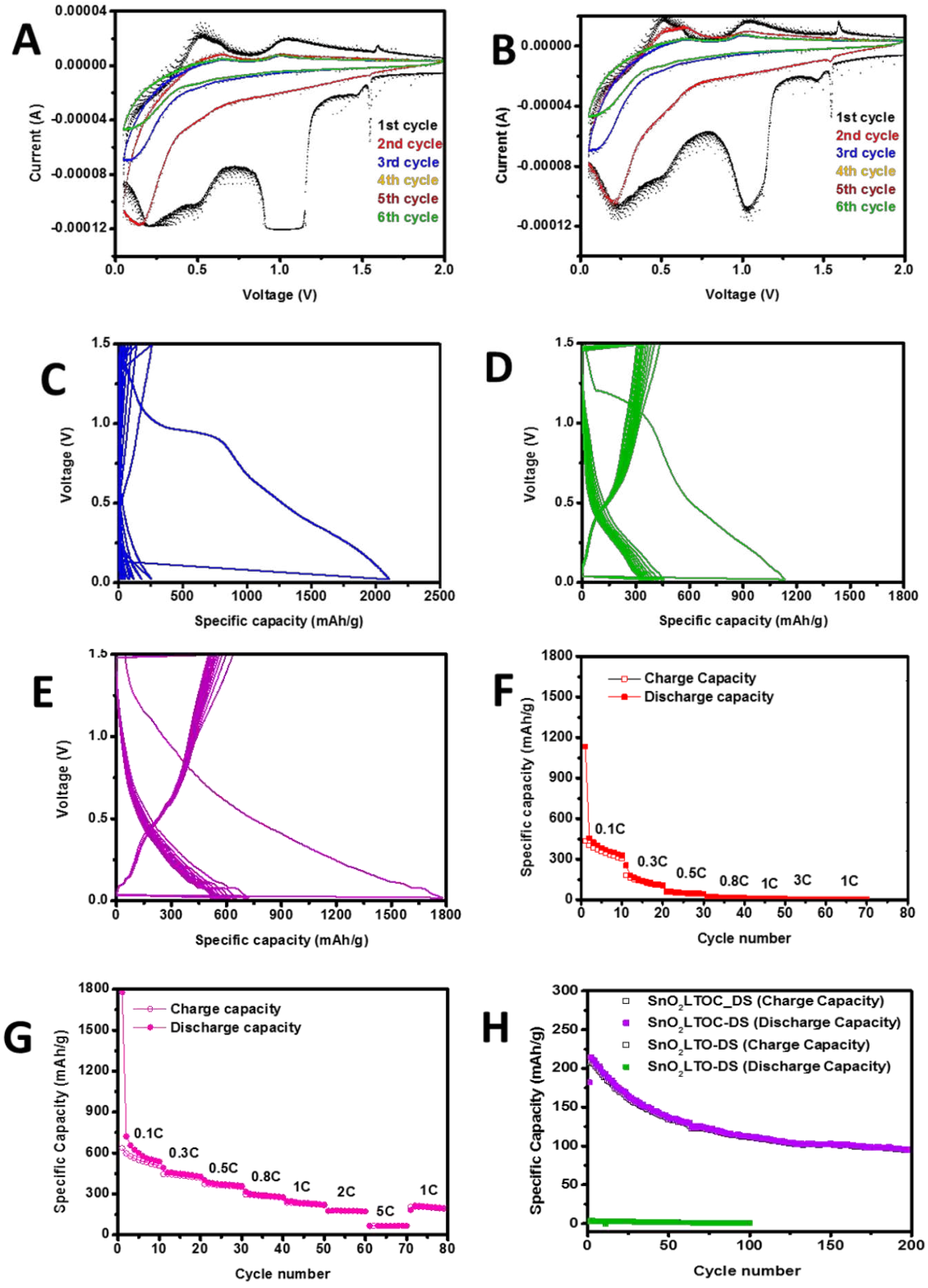

Figure 2: Cyclic Voltammetry studies of SnO_2LTO-DS (A) and SnO_2LTOC-DS (B) at 0.05 mV/s for six cycles. C, D, and E depicts voltage profile of SnO_2 powders, SnO_2LTO-DS and SnO_2LTOC-DS respectively at 0.1C rates. F and G in the figure represents the rate performance study of SnO_2LTO-DS and SnO_2LTOC-DS at varying C

rates. The GCD cycle stability studies of SnO_2LTO-DS and SnO_2LTOC-DS at 1C rate after the rate capability studies are represented in H.

TABLE I. A summary of galvanostatic charge discharge studies.

Type of electrode	Capacity after initial 10 cycles (mAh/g)	Capacity after rate capability studies (mAh/g)	Capacity after 200 cycles of cycle stability studies (mAh/g)	Percentage capacity loss in cycle stability studies (%)
SnO_2-P	0	-	-	-
SnO_2LTO-DS	300	0	98	56
SnO_2LTOC-DS	517	215	0	99

References

[1] J.S. Chen, X. Wen, D. Lou, *Small*, **11**, 1877 (2013).
[2] J. Zhang, L.B. Chen, C.C. Li, T.H. Wang, *Appl. Phys. Lett.* **93**, 1 (2008).
[3] J. Zhu, Z. Lu, S.T. Aruna, D. Aurbach, A. Gedanken, *Chemi. Mater.* **12,** 2557 (2000).
[4] C.K. Chan, H. Peng, G. Liu, K. McIlwrath, X.F. Zhang, R.A. Huggins, Y. Cui, *Nat. Nanotechnol.* **3,** 31(2008).
[5] H. Wu, G. Chan, J.W. Choi, I. Ryu, Y. Yao, M.T. Mcdowell, S. Woo, A. Jackson, L. Hu, Y. Cui, *Nat. Nanotechnol.* **7** 310 (2012)
[6] N.-S. Choi, Y. Yao, Y. Cui, J. Cho, *J. Mat. Chem.* **21** 9825 (2011)
[7] P. Meduri, C. Pendyala, V. Kumar, G.U. Sumanasekera, M.K. Sunkara, *Nano Lett.* **9** 612 (2009)
[8] H. Wang, G. Liu, Z. Yang, B. Wang, L. Chen, Q. Jiang, *Int. J. Electrochem. Sci.* **8** 2345 (2013)
[9] S. Chen, M. Wang, J. Ye, J. Cai, Y. Ma, H. Zhou, L. Qi, *Nano Res.* **6**, 243 (2013)
[10] R. Liu, N. Li, D. Li, G. Xia, Y. Zhu, S. Yu, C. Wang, *Mat. Lett.* **73**, 1(2012)
[11]L. Zou, L. Gan, F. Kang, M. Wang, W. Shen, Z. Huang, *J. Power sources* **195**, 1216(2010).
[12] L.B. Chen, X.M. Yin, L. Mei, C.C. Li, D.N. Lei, M. Zhang, Q.H. Li, Z. Xu, C.M. Xu, T.H. Wang, *Nanotechnology* **23,** 1(2012).
[13] G. Chen, Z. Wang, D. Xia, One-pot synthesis of carbon nanotube @ SnO2 – Au coaxial nanocable for lithium-ion batteries with high rate capability, Chem. Mater 20 (2008) 6951e6956.
[14] X. Ji, X. Huang, J. Liu, *Nanoscale Res. Lett.* **5,** 649 (2010).
[15] P. Wu, N. Du, H. Zhang, J. Yu, D. Yang, *J. Phys. Chem. C* **114**, 22535 (2010)
[16] J.M. Chem, Z. Zhang, R. Zou, G. Song, L. Yu, Z. Chen, J. Hu, *J. Mat. Chem.* **21** 17360 (2011)
[17] Q. Guo, Z. Zheng, H. Gao, J. Ma, X. Qin, *J. Power sources* **240,** 149 (2013)
[18] X. Hou, X. Wang, B. Liu, Q. Wang, Z. Wang, D. Chen, *Chem. Electro Chem.* **1,** 108 (2014).
[19] M.H. Kim, Y.C. Kang, *Int. J. Electrochem. Sci.* **8**, 3676 (2013)
[20] J.M. Chem, Y. Lin, R.K. Nagarale, K.C. Klavetter, C.B. Mullins, *J. Mat. Chem.* **8** 11134 (2012).
[21] K.M. Yang, Y.J. Hong, S.H. Choi, B.K. Park, Y.C. Kang, *Int. J. Electrochem Sci.* **8**, 1026 (2013)

[22] G. Ji, Y. Ma, B. Ding, J.Y. Lee, *Chem. Mater*. **24**, 3329 (2012).
[23] R. Cai, X. Yu, X. Liu, Z. Shao, *J. Power Sources* **195**, 8244 (2010).
[24] Y.-Y. Wang, Y.-J. Hao, Q.-Y. Lai, J.-Z. Lu, Y.-D. Chen, X.-Y. Ji, *Ionics* **14,** 85 (2008)
[25] X. Li-zhi, H.E. Ze-qiang, Y. Z-lan, Q.-Y. Chen, *Trans. Nonferrous Met. Soc. China* **20,** 270 (2010).
[26] Y- J. Hao, Q.-Y. Lai, Y.-D. Chen, J.-Z. Lu, X.-Y. Ji, *J. Alloys Compd.* **462**, 404 (2008)
[27] K. M. Yang, Y.C. Kang, S.M. Jeong, Y.J. Choi, Y.S. Kim, *Int. J. Electrochem. Sci.* **8**, 11972 (2013)
[28] A. K. Haridas, C. S. Sharma N. Y. Hebalkar, T. N. Rao, *Materials Today Energy,* **4**, 14 (2017).
[29] A.K. Haridas, C.S. Sharma, T.N. Rao, *Small,* **11,** 290 (2015).
[30] A.K. Haridas, C.S. Sharma, T.N. Rao, *Electroanaysis*, **26**, 2315, (2014).
[31] X. Li-zhi, H.E. Ze-qiang, Y. Z-lan, Q.-Y. Chen, *Trans. Nonferrous Met. Soc. China* **20,** s267 (2010).
[32] X.M. Yin, C.C. Li, M. Zhang, Q.Y. Hao, S. Liu, L.B. Chen, T.H. Wang, *J. Phys.Chem.C* **114,** 8084, (2010).
[33] J. Chen, K. Yano, *ACS Appl. Mat. Interfaces,* **5**, 768 (2013).